Final Report for Period: 09/2005 - 09/2006
Submitted on: 11/22/2006
Principal Investigator: Garcia, Andres J.
Award ID: 0093226
Organization: GA Tech Res Corp - GIT
Title:
CAREER: Hybrid Surfaces to Control Cell Adhesion and Function

Project Participants

Senior Personnel

Name: Garcia, Andres
Worked for more than 160 Hours: Yes
Contribution to Project:

Post-doc

Graduate Student

Name: Gallant, Nathan
Worked for more than 160 Hours: Yes
Contribution to Project:
Responsible for developing micropatterned surfaces and related cell adhesion analyses.

Name: Cutler, Sarah
Worked for more than 160 Hours: Yes
Contribution to Project:
Responsible for developing immobilization scheme to create fibronectin-mimetic surfaces and related cell adhesion analyses.

Name: Capadona, Jeffrey
Worked for more than 160 Hours: Yes
Contribution to Project:
Responsible for synthesis of functionalized alkanethiols and protein adsorption and cell adhesion analyses.

Name: Cao, Tim
Worked for more than 160 Hours: Yes
Contribution to Project:
Responsible for micropatterning surfaces to immobilize controlled ligand densities.

Name: Petrie, Tim
Worked for more than 160 Hours: Yes
Contribution to Project:
Tim has been working on expressing the bioactive ligand in the PinPoint system.

Undergraduate Student

Name: Berguig, Geoffrey
Worked for more than 160 Hours: Yes
Contribution to Project:
Mr. Berguig constructed and validated a photolithography system to generate micropattered cell culture arrays.

Technician, Programmer

Other Participant

Name: Steele, Katrina
Worked for more than 160 Hours: Yes
Contribution to Project:
Responsible for extending protein stamping technique to neuronal cell culture.

Research Experience for Undergraduates

Name: von Reyn, Catherine
Worked for more than 160 Hours: No
Contribution to Project:
Responsible for model micropatterning surfaces to immobilize controlled ligand densities.

Years of schooling completed: Junior
Home Institution: Same as Research Site
Home Institution if Other:
Home Institution Highest Degree Granted(in fields supported by NSF): Doctoral Degree
Fiscal year(s) REU Participant supported: 2003
REU Funding: No Info

Name: Creighton, Francis
Worked for more than 160 Hours: No
Contribution to Project:

Years of schooling completed: Sophomore
Home Institution: Same as Research Site
Home Institution if Other:
Home Institution Highest Degree Granted(in fields supported by NSF): Doctoral Degree
Fiscal year(s) REU Participant supported: 2005
REU Funding: No Info

Name: Willis, TaRessa
Worked for more than 160 Hours: Yes
Contribution to Project:
Ms. Willis worked on designing a custom-made photolithography system to generate micropatterned surfaces.

Years of schooling completed: Junior
Home Institution: Same as Research Site
Home Institution if Other:
Home Institution Highest Degree Granted(in fields supported by NSF): Doctoral Degree
Fiscal year(s) REU Participant supported: 2005
REU Funding: REU supplement

Organizational Partners

Other Collaborators or Contacts

David Collard (Chemistry, GATech) provided expertise on synthesis and characterization of alkanethiols.

A.Bruno Frazier (Electrical Engineering, GATech) provided expertise on micropatterned mold fabrication.

Harold Erickson (Duke Univ.) provided bacteria transformed with fibronecitn fragment.

Robert Latour (Clemson Univ.) provided ellipsometry measurements for tethered ligands.

Activities and Findings

Research and Education Activities: (See PDF version submitted by PI at the end of the report)

Findings:

The major findings in Year 1 relate to the development of (1) micropatterned surfaces to modulate cell adhesion, shape, and assembly of focal adhesions, and (2) a biofunctionalization strategy to generate fibronectin-mimetic surfaces that support specific integrin binding and cell adhesion. These results demonstrate that we can engineer biospecific surfaces to control cell adhesion. In particular, these biomolecular strategies exhibit significant advantages over current biomaterial approaches to manipulate cell adhesion and function in terms of controlled ligand densities, integrin specificity, and controlled cell spreading and focal adhesion area.

The major findings in Year 2 relate to the development of (i) FN-mimetic surfaces to control integrin binding, (ii) protein-resistant surfaces with anchoring groups onto which adhesive ligands can be immobilized in a controlled fashion, and (iii) micropatterned surfaces presenting controlled ligand densities. These findings establish approaches for the engineering of robust biomimetic surfaces to control cell adhesion and function. These results are critical to our ultimate objective of analyzing the contributions of integrin binding and focal adhesion area/cell spreading to osteoblastic cell differentiation.

The major findings in Year 3 relate to (i) ligand tethering to non-fouling synthetic surfaces and (ii) synthetic surfaces promoting fibronectin matrix assembly. These findings establish approaches for the engineering of robust biomimetic surfaces and demonstrate novel biomimetic strategies to control matrix assembly. These results are critical to our ultimate objective of controlling cell functions through the underlying substrate.

The major findings in Year 4 relate to (i) engineering surfaces that nucleate and template extracellular matrix assembly and (ii) developed techniques to prepare micropatterned domains presenting controlled bioligand densities. These findings establish approaches for the engineering of robust biomimetic surfaces and demonstrate novel biomimetic strategies to control matrix assembly. These results are critical to our ultimate objective of controlling cell functions through the underlying substrate.

The major findings in Year 5 constitute the engineering of synthetic surfaces that present biomimetic adhesive motifs that convey integrin binding specificity and signaling. We also validate a general methodology applicable to the analysis of biomimetic peptides for the functionalization of biomaterials. These findings establish strategies targeting specific integrin adhesion receptors as promising approaches for the engineering of bioactive materials that control cellular responses.

Training and Development:

In year 1, this project has provided research training for three bioengineering graduate students, particularly in surface preparation/characterization and cell adhesion analyses. In addition, this project, as part of an REU supplement to our ERC on the Engineering of Living Tissues, provided an undergraduate student in biology with an intensive research experience in an innovative area of bioengineering.

In year 2, this project has provided research training for two bioengineering graduate students, particularly in surface engineering and cell adhesion analyses. In addition, we are currently hosting an REU student working on initial micropatterning studies with controlled ligand densities.

In year 3, this project has provided research training for two bioengineering graduate students, particularly in surface engineering and cell adhesion analyses.

In year 4, this project has provided research training for two bioengineering graduate students as well as a REU student.

In year 5, this project provided research training for one bioengineering graduate student and two undergraduate students.

Outreach Activities:

An important educational component of this project is the development of middle school science Web-based module on receptor-ligand interactions ('Receptor Guy'). The module, written in Macromedia's Director, has been packaged as a Flash file on CD-ROMs and distributed to several middle-school science teachers in local public and private schools for initial feedback and evaluation. In addition to changes to the current module, we anticipate comments/suggestions to integrate into the next module.

In year 2, an important educational component of this project is the development of middle school science Web-based module on receptor-ligand interactions ('Receptor Guy'). We have met with several middle-school science teachers from area schools and obtained feedback on improvements to the module and content for future modules. We are currently working on integrating the module into the science curriculum in Atlanta Public School and Dekalb County School districts.

We have developed a second generation of the proposed middle school science Web-based module on receptor-ligand interactions ('Receptor Guy'). Over the last year, we have met with several middle-school science teachers from Atlanta Public School and Dekalb County School districts and obtained feedback on improvements to the module and content for future modules. The Georgia Public School Science curriculum is currently undergoing a major evaluation and we are discussing implementation of these modules into the curriculum. We have identified several challenges to integrating the module into the science curriculum including teacher training and support, wide distribution of modules, integration into coursework, and manpower and resources associated with the development and implementation of these modules. We have also discussed the possibility of creating 'hands on' kits or demonstration units to complement science courses. These kits offer significant advantages compared to the modules in terms of simplicity and impact. Finally, we are hosting nine high school students from Campbell High School in independent research projects focusing on drug delivery. These students are conducting experiments on parameters controlling release of model drugs (food coloring dyes) from hydrogels (gelatin).

We have met with several middle-school science teachers from Atlanta Public Schools to discuss improvements to the module and content for future modules. We identified several challenges to integrating the module into the science curriculum including teacher training and support, wide distribution of modules, integration into coursework, and manpower and resources associated with the development and implementation of these modules. We have also met with representatives from the Fernbank Museum of Natural History to discuss possible integration of our research into their science and outreach programs. Both the middle-school teachers and Fernbank representatives were excited by the idea of creating kits or demonstration units to complement science courses.

In addition to these science kits, we are currently discussing creating a one-week science camp module focusing on biomaterials. This module would provide hands-on and problem-based learning experiences for middle school students.

Journal Publications

Gallant, N.D., Capadona, J.R., Frazier, A.B., Collard, D.M., and GarcÝa, A.J., "Micropatterned surfaces for analyzing cell adhesion strengthening", Langmuir, p. , vol. , ( ). Accepted

Cutler, S.M. and García, A.J., "Engineering cell adhesive surfaces that direct integrin alpha5beta1 binding using a recombinant fragment of fibronectin", Biomaterials, p. 1759, vol. 24, (2003). Published

Capadona, J.R., Collard, D.M., and GarcÝa, A.J., "Fibronectin adsorption and cell adhesion to mixed monolayers of tri(ethylene glycol)- and methyl-terminated alkanethiols", Langmuir, p. 1847, vol. 19, (2003). Published

Garcia, A.J. and Gallant, N.D., "Stick and Grip: Measurement systems and quantitative analyses of integrin-mediated cell adhesion strength", Cell Biochemistry and Biophysics, p. 61, vol. 39, (2003). Published

Capadona JR, Petrie TA, Fears KP, Latour RA, Collard DM, García AJ, "Surface-nucleated assembly of fibrillar extracellular matrices", Advanced Materials, p. 2604, vol. 17, (2005). Published

Garcia AJ, "Interfaces to Control Cell-Biomaterial Adhesive Interactions", Advances in Polymer Science, p. 171, vol. 203, (2006). Published

Petrie TA, Capadona JR, Reyes CD, Garcia AJ, "Integrin specificity and enhanced cellular activities associated with surfaces presenting a recombinant fibronectin fragment compared to RGD supports", Biomaterials, p. 5459, vol. 27, (2006). Published

Garcia AJ, "Get a grip: integrins in cell?biomaterial interactions", Biomaterials, p. 7525, vol. 26, (2005). Published

Garcia AJ, Reyes CD, "Bio-adhesive surfaces to promote osteoblast differentiation and bone formation", J Dent Res, p. 407, vol. 84, (2005). Published

Gallant ND, Charest JL, King WP, Garcia AJ, "Micro- and Nano-Patterned Substrates to Manipulate Cell Adhesion", J Nanosci Nanotechnol, p. 1, vol. 7, (2007). Published

Books or Other One-time Publications

GarcÝa, A.J. and Keselowsky, B.G., "Biomimetic surfaces for control of cell adhesion to facilitate bone formation", ( ). Book, Accepted
Editor(s): Stein, G.S., and Lian, J.B.
Bibliography: Critical Reviews in Eukaryotic Gene Expression, Volume 12, Issue 02

Garcia, A.J., "Biomimetic materials", (2006). book chapter, Published
Editor(s): Bronzino
Collection: The Biomedical Engineering Handbook

Bibliography: Tissue Engineering and Artificial Organs, Third Editions, CRC Taylor & Francis, Boca Raton

Web/Internet Site

Other Specific Products

Contributions

Contributions within Discipline:
We have developed surface engineering strategies to control specific integrin binding and cell spreading and focal adhesion area. These approaches may be useful to manipulate cell adhesion and function in numerous applications. We have also engineered surfaces that direct matrix assembly.

Contributions to Other Disciplines:

Contributions to Human Resource Development:

Contributions to Resources for Research and Education:

Contributions Beyond Science and Engineering:

Categories for which nothing is reported:

Organizational Partners
Any Web/Internet Site
Any Product
Contributions: To Any Other Disciplines
Contributions: To Any Human Resource Development
Contributions: To Any Resources for Research and Education
Contributions: To Any Beyond Science and Engineering

Project Objectives

This project integrates innovative research and educational initiatives focusing on the **engineering of bioadhesive surfaces to control cell function driven by a mechanistic understanding of adhesion receptor-ligand interactions**. Receptor-ligand interactions govern a variety of cellular functions, including adhesion, signaling, proliferation, and differentiation. In particular, receptor-mediated cell adhesion to extracellular matrix (ECM) proteins provides tissue structure and triggers signals that direct cell proliferation and differentiation. Due to its central role in development, tissue remodeling, and wound healing, cell adhesion is crucial to many biomedical and biotechnological applications. Cell adhesion to ECM proteins is primarily mediated by integrins, a widely expressed family of receptors. In addition to anchoring cells, integrins provide signals critical for growth and differentiation. Binding of integrins to their ligands is governed by interactions with specific amino acid sequences in the ligand. **The research objective of this project is to engineer bioadhesive surfaces inspired by fibronectin (FN), an essential and ubiquitous ECM protein, to control cell adhesion in order to direct cell differentiation**. This project focuses on two aspects of cell adhesion, integrin binding and cell spreading, which are critical to cell function. This overall objective is addressed by the following specific aims:

1. **To engineer hybrid surfaces presenting well-defined ligand densities that exhibit high affinity for particular integrin receptors and control cell spreading**. Synthetic surfaces (self-assembled monolayers of alkanethiols) will be functionalized with recombinant fragments of FN and micropatterning techniques will be applied to modulate cell spreading.
2. **To analyze cell adhesion to the engineered surfaces as a function of ligand density and available spreading area.** Cell adhesion will be analyzed in terms of integrin binding, adhesion strength, intracellular signaling, and focal adhesion and cytoskeleton assembly.
3. **To investigate the effects of specific integrin binding and cell spreading on cell differentiation.** This project will focus on the differentiation of osteoblasts (bone forming cells), in particular bone-specific gene expression and matrix mineralization, as a model system.

This project is directly relevant to multiple biotechnological and biomedical applications, including in vitro culture systems, biomaterials, and tissue engineering, as well as fundamental cell biology. Development of bioactive surfaces to direct cell function is central to biomaterials and tissue engineered scaffolds for enhanced repair. For instance, engineering of surfaces to promote bone cell differentiation and matrix mineralization is important to the osseointegration of orthopaedic and dental implants and bone grafting scaffolds. In addition, the ability to express differentiated phenotypes in vitro is critical to basic studies focusing on tissue-specific gene expression and drug efficacy and toxicity in differentiated cell types. Finally, engineering of surfaces that control adhesive interactions is important to fundamental studies of cell adhesion, such as the role of integrin clustering and cytoskeletal assembly in adhesion strengthening.

Because of the central role of receptor-ligand interactions in cellular engineering, **the educational component of this proposal focuses on the development of interactive Web-based modules to model receptor-ligand interactions for (i) middle school science and (ii) graduate-level cellular engineering courses**. These two separate modeling platforms will provide versatile "hands-on" instructional tools. Integration of this instructional technology with conventional lectures and laboratory exercises will promote enhancement of the learning process. These modules also allow for the integration of research into the educational experience and permit "virtual" experimentation that is not possible in conventional laboratory settings. The modular format of the platforms allows for flexibility in the depth and complexity of the material for different instructional levels, while the Web-based format provides for wide dissemination.

Research Activities

1. Cell Adhesion to Micropatterned Surfaces

Microcontact printing was used to pattern self-assembled monolayers (SAMs) of alkanethiols into adhesive and non-adhesive domains. Long-chain alkanethiols ($HS\text{-}[CH_2]_n\text{-}X$, where $n \geq 10$ and X is the tail group) adsorb from solution onto Au to form stable, well packed and ordered monolayers. The sulfur on the

chain head coordinates strongly to Au and the trans-extended alkyl chain presents the tail group X at the SAM-solution interface. The tail group controls the physicochemical properties of the SAM, allowing tailoring of specific surface chemistries such as groups that resist protein adsorption or moieties that can be modified to immobilize peptides and proteins. Furthermore, surfaces of mixed composition can be engineered by co-adsorption of different alkanethiols, providing a simple and robust system to generate multi-component surfaces of varying compositions. Using standard photolithography methods, we manufactured master templates of microarrays of different circular islands (2, 5, 10 μm dia.; 75 μm center-to-center spacing) on Si wafers. Poly(dimethylsiloxane) stamps were then cast from these templates and used to micropattern substrates on Au-coated glass coverslips. Briefly, the face of the stamp was inked with 1 mM ethanolic solution of hexadecanethiol ($HS\text{-}[CH_2]_{17}\text{-}CH_3$) and brought into conformal contact with the Au-coated substrate for 15 seconds to produce an array of circular islands of a hydrophobic SAM to which proteins readily adsorb. Subsequently, the coverslips were incubated in a 2 mM ethanolic solution of tri(ethylene glycol)-terminated alkanethiol ($HS\text{-}[CH_2]_{12}\text{-}[OCH_2CH_2]_3OH$) for 16 hours to create a non-fouling and non-adhesive background around the CH_3-terminated islands. Finally, micropatterned substrates were coated with FN (10 μg/ml in PBS) for 1 hour and blocked with 1% serum albumin for 1 hour. NIH3T3 fibroblasts were seeded on micropatterned substrates at 225 cells/mm^2 in serum-containing media.

Functional micropatterning was confirmed by staining with FN-specific antibodies, demonstrating that FN preferentially adsorbed onto the circular islands (**Fig. 1**). NIH3T3 fibroblasts were used to investigate cell-micropatterned substrate interactions. These cells were selected because this continuous cell line has been extensively characterized in terms of its adhesive properties (integrin expression, focal adhesion assembly, spreading). Cells adhered to FN-coated micropatterned islands and remained constrained to the available spreading area (**Fig. 1**). Cells maintained a round morphology and there were no gross differences in morphology among the micropatterned islands, although cells adhering to 10 μm islands appeared more hemispherical than cells on the smaller islands, as expected for the larger available spreading area. NIH3T3 cells remained viable and attached to the substrates for up to 5 days in culture for all FN-coated micropatterned island sizes.

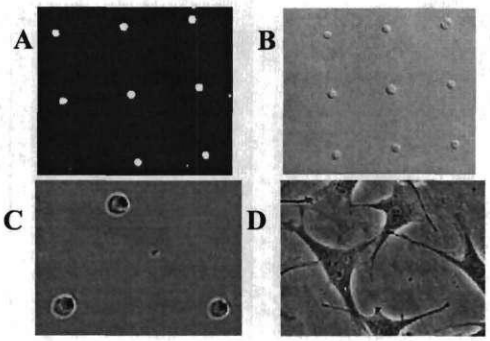

Fig. 1: Micropatterned surfaces that control protein adsorption and cell spreading. (**A**) Immunofluorescence staining for FN showing selective adsorption onto adhesive areas (10 μm dia. islands). (**B**) NIH3T3 adhesion and spreading (5 μm dia. islands) at 2 days. (**C**) Phase contrast micrograph of cells on (**C**) patterned and (**D**) unpatterned substrates.

Assembly of focal adhesion complexes was examined for all substrates at 16 hours in culture by immunofluorescence staining. Cells adhering to FN-coated, unpatterned CH_3-terminated SAMs spread and exhibited characteristic focal adhesion complexes consisting of discrete spear-like structures (0.1-1 μm long) containing clustered integrin $\alpha_5\beta_1$ and cytoskeletal elements, including vinculin, talin, α-actinin and paxillin (**Fig. 2A**). For all micropatterned substrates, adhesive structures were localized to a central circular region constrained to the micropatterned island (**Fig. 2B, C**). These adhesive structures resembled conventional focal adhesions in their composition as integrin $\alpha_5\beta_1$, vinculin, talin, α-actinin and paxillin were all localized to the adhesive structures on the micropatterned islands. For 10 μm diameter islands, integrin receptors, although still constrained to the adhesive island, were spatially segregated into discrete clusters while other regions within the adhesive domain appeared devoid of adhesion receptors (**Fig. 2B**), analogous to the morphology observed for conventional focal adhesions. Analysis of these immunostained images revealed that clustered integrins occupied approximately 60% of the available adhesive domain. Cytoskeletal proteins

also exhibited similar distributions within the adhesive domain and co-localized with integrin receptors (**Fig. 2C**). In contrast, for 2 and 5 μm diameter islands, bound integrins exhibited a more uniform distribution across the micropatterned adhesive domain and no distinct spear-like discrete clusters or areas devoid of bound integrins were observed (**Fig. 2B**). Image analysis revealed greater than 95% coverage of the available adhesive area. Interestingly, for these smaller patterns, cytoskeletal components (vinculin, talin) were present throughout the entire adhesive island but displayed enriched concentration at the periphery compared to the center of the adhesive island (**Fig. 2C**). Taken together, these immunostaining results demonstrate that micropatterning approaches can be applied to engineer adhesive domains and focal adhesion assembly while controlling overall cell shape.

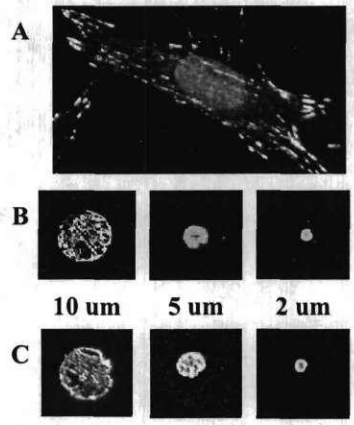

Fig. 2: Localization of focal adhesion components to micropatterned islands at 16 hr as visualized by immunofluorescence staining. (**A**) Focal adhesions (vinculin) for cell on unpatterned CH_3-SAM show characteristic spear-like clustered morphology. (**B**) Bound integrin $\alpha_5\beta_1$ in NIH3T3 cells adhering to micropatterned islands (10 μm, 5 μm and 2 μm dia.). (**C**) Cytoskeletal protein talin localized to micropatterned islands.

Cell adhesion strength to FN-coated micropatterned islands was quantified using a spinning disk device previously characterized by our group. This system applies a well-defined range of hydrodynamic forces to adherent cells and provides sensitive measurements of adhesion strength. For all micropatterned substrates, cell adhesion strength increased rapidly at early time points and reached plateau values by 4 hr (**Fig. 3**). Comparison of experiments for similar contact areas at different time points (15 min vs. 16 hour) showed a 9-fold increase in adhesion strength over time, independently of cell spreading and redistribution of adhesive structures to the cell periphery. We examined the functional dependence of adhesion strength on available contact area by comparing steady state values (16 hr) for different adhesive island dimensions. As expected, adhesion strength increased with island diameter (**Fig. 4**), indicating that focal adhesion area strongly modulates adhesion strength. Increasing adhesive area from 3.1 μm^2 (2 μm dia.) to 19.6 μm^2 (5 μm dia.) resulted in a 2-fold increase in adhesion strength, whereas a subsequent 4-fold increase in adhesive area to 78.5 μm^2 (10 μm dia.) produced a 20% enhancement in strength. Due to non-uniform bond loading in the

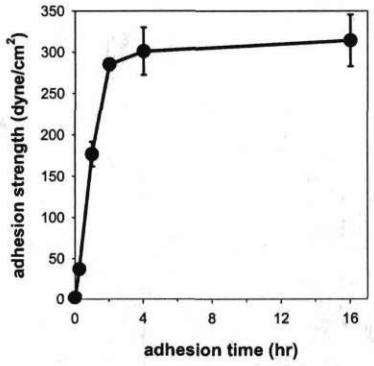

Fig. 3: NIH3T3 adhesion strength (mean ± std. error) as a function of time on 5 μm dia. islands showing rapid increases in initial strength and reaching saturation values at 4 hr.

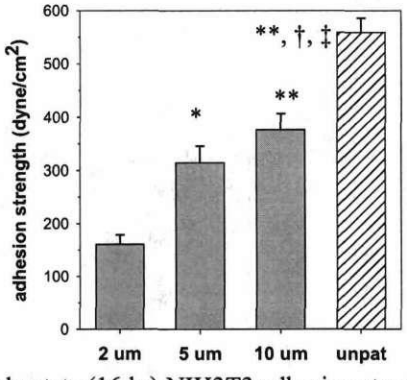

Fig. 4: Steady-state (16 hr) NIH3T3 adhesion strength (mean ± std. error) for different adhesive island diameters showing contact area-dependent values (ANOVA $p < 0.00002$; * 5 μm > 2 μm ($p < 0.003$); ** unpat, 10 μm > 2 μm ($p < 0.0004$); † unpat > 5 μm ($p < 0.00005$); ‡ unpat > 10 μm ($p < 0.002$)).

contact area, we do not expect a one-to-one correspondence between adhesive area and adhesion strength, and we attribute these differences in adhesion strength enhancement to differences in focal adhesion area.

These results demonstrate that microcontact printing of SAMs can be used to control cell shape and engineer focal adhesion position and size. This micropatterning approach provides a robust strategy to decouple focal adhesion assembly from cell spreading for the analysis of structure-function relationships in adhesive interactions. By combining these micropatterned surfaces with our quantitative cell adhesion assay, we demonstrated time- and contact area-dependent increases in cell adhesion strength. Furthermore, we showed that focal adhesion assembly contributes significantly to adhesion strengthening independently of cell spreading and redistribution of adhesive structures. This work provides an experimental framework for the functional analysis of focal adhesion structural and signaling components.

2. FN-mimetic Surfaces Promoting Binding of $\alpha_5\beta_1$ Integrin

We have engineered surfaces that promote binding of $\alpha_5\beta_1$ because this integrin is central to osteoblastic activities. Binding of $\alpha_5\beta_1$ requires both the RGD and PHSRN sites in FN and short RGD peptides do not support $\alpha_5\beta_1$ binding (García et al., *Biochemistry* 41: 9063-69, 2002). Our biomimetic strategy focuses on a recombinant fragment of FN (FNIII7-10) that encompasses the PHSRN and RGD binding domains and exhibits biological activities equivalent to plasma FN. The use of a recombinant protein offers several advantages over the native molecule, including reduced antigenicity, elimination of domains that may elicit adverse reactions (e.g. complement- and fibrinogen-binding domains), and enhanced cost efficiency. Recombinant technology also provides flexibility in introducing specific residues via site-directed mutagenesis to enhance protein immobilization and activity. We have engineered model FN-mimetic surfaces by immobilizing FNIII7-10 onto passively adsorbed, non-adhesive albumin. Homo- and hetero-bifunctional cross-linkers of varying spacer-arm length targeting either available cysteine or lysine groups on FNIII7-10 were investigated in ELISA and cell adhesion assays to optimize immobilization densities and activity. FN-mimetic surfaces presenting controlled densities of FNIII7-10 were engineered by varying the concentration of FNIII7-10 in the coupling solution at a constant cross-linker concentration (**Fig. 5**). Cells adhered to these functionalized surfaces via $\alpha_5\beta_1$ as shown by blocking with integrin-specific antibodies (**Fig. 6**). In addition, cells spread and assembled focal adhesions containing $\alpha_5\beta_1$, vinculin, and talin (**Fig. 6**). These results demonstrate the ability to engineer surfaces that bind specific integrin receptors. Although these surfaces provided precise control of integrin binding and cell adhesion, these substrates are limited to short term studies (< 4 h) because the albumin support is reorganized by cells. We have extended this work to more robust synthetic supports (see below).

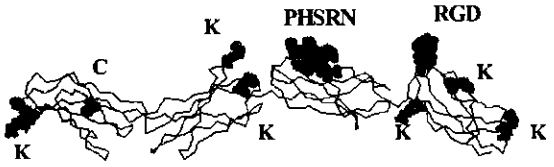

Fig. 5: FN-mimetic surfaces. Model of FNIII7-10 showing RGD and PHSRN sites and lysine (K) and cysteine (C) available for immobilization. FNIII7-10 immobilized density (detected by HFN7.1 antibody) as a function of solution concentration for two amine-reactive cross-linkers. Passive adsorption onto synthetic support is shown for reference.

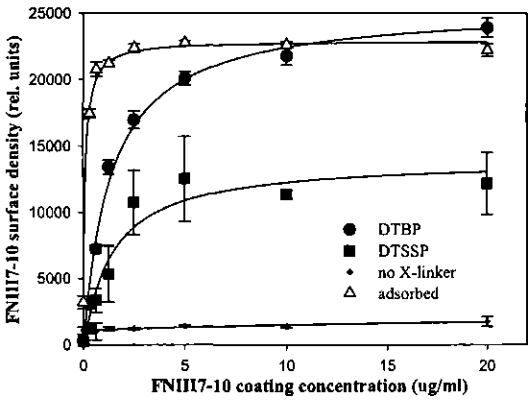

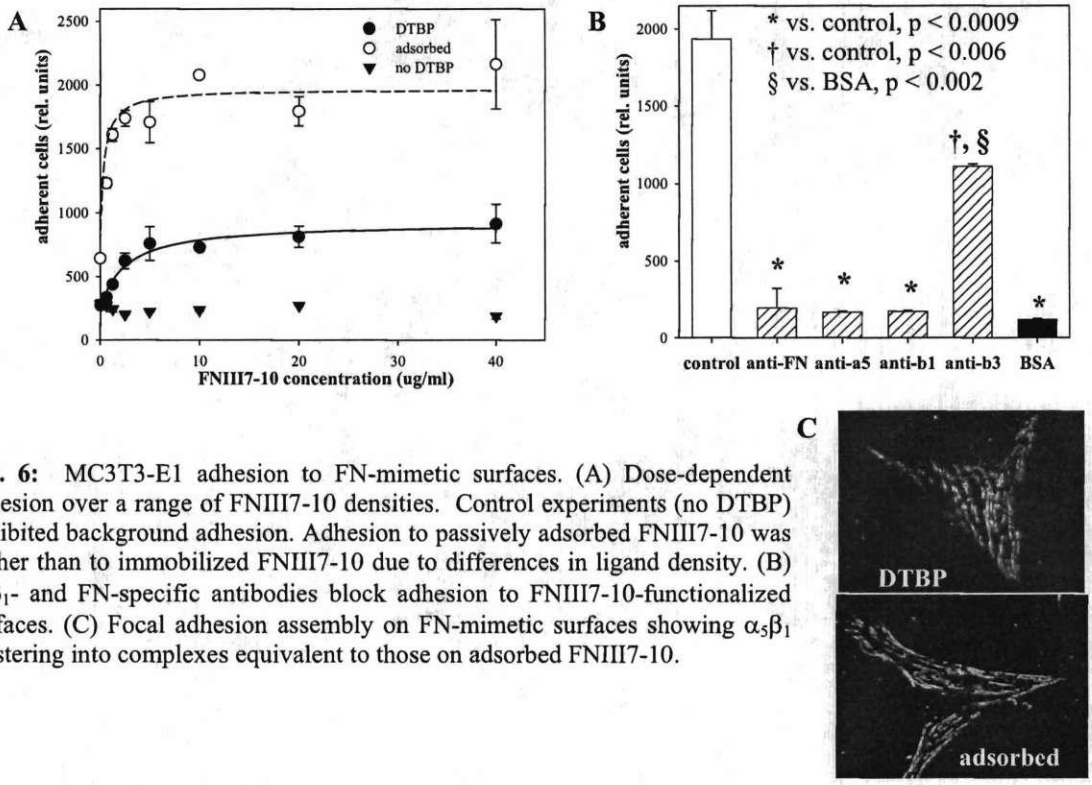

Fig. 6: MC3T3-E1 adhesion to FN-mimetic surfaces. (A) Dose-dependent adhesion over a range of FNIII7-10 densities. Control experiments (no DTBP) exhibited background adhesion. Adhesion to passively adsorbed FNIII7-10 was higher than to immobilized FNIII7-10 due to differences in ligand density. (B) $\alpha_5\beta_1$- and FN-specific antibodies block adhesion to FNIII7-10-functionalized surfaces. (C) Focal adhesion assembly on FN-mimetic surfaces showing $\alpha_5\beta_1$ clustering into complexes equivalent to those on adsorbed FNIII7-10.

3. Ligand Tethering to Non-fouling Synthetic Surfaces

We have synthesized two alkanethiols to engineer stable, non-fouling surfaces presenting controlled adhesive ligand densities: EG_3-terminated thiol [$HS(CH_2)_{11}(OCH_2CH_2)_3OH$] and EG_6COOH-terminated thiol [$HS(CH_2)_{11}(OCH_2CH_2)_6OCH_2CO_2H$] (**Fig. 7**). We used these thiols to generate uniform SAMs to tether bioactive ligands. This system has been validated for immobilization of a variety of peptides and proteins by Whitesides and colleagues (Lahiri et al., *Anal Chem* 71, 777-790, 1999). Mixed SAMs were prepared by immersing Au substrates in alkanethiol solutions for 4h. The solution consisted of 95% 1 mM $HS(CH_2)_{11}$-$(OCH_2CH_2)_3OH$ (EG_3) and 5% 1 mM $HS(CH_2)_{11}$-$(OCH_2CH_2)_6OCH_2CO_2H$ (EG_6-COOH). Thiols were synthesized as previously described and characterized by ^1H- and ^{13}C-NMR, FT-IR, and mass spectroscopy. Ligand immobilization was performed using standard EDC chemistry. SAM carboxylic acids were converted to active NHS-esters by incubating for 30 min in 2 mM EDC (1-ethyl-3-(3-dimethylaminopropyl)carbodiimide hydrochloride) and 5 mM NHS (*N*-hydroxysuccinimide) in 0.1 M MES (2-(N-morpholino)-ethanesulfonic acid) and 0.5 M NaCl, pH 6.0. NHS- esters reacts with primary amines in the ligand. Different concentrations of ligand were incubated on the activated surface in coupling buffer (0.1 M MES, 0.5 M NaCl, pH 6.0) for 30 min. The reaction was quenched with 20 mM 2-mercaptoethanol for 5 min. Surface reactions were monitored by polarized infrared external reflectance spectrometry (PIERS) and tethered ligand densities were quantified via enzyme-linked immunosorbent assays (ELISA).

Fig. 7: Functionalized alkanethiols used to create SAMs

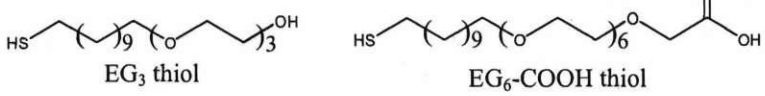

EG_3 thiol $\qquad$ EG_6-COOH thiol

Transformation of the SAM carboxylic acid to the reactive NHS-ester was characterized by PIERS. **Fig. 8** shows PIERS spectra for representative surface reaction stages. Pure EG_3 SAMs displayed no peaks in the carbonyl region of the spectrum, consistent with its molecular structure. SAMs consisting of 95% EG_3 and 5% EG_6-COOH showed a large sharp peak at 1621 cm^{-1} which is assigned to the carbon-oxygen double bond stretch signiture to carboxylic acids. After activation with EDC and NHS, the 1621 cm^{-1} peak was reduded

indicating convertion of the acid. Newly formed peaks at 1741 cm^{-1}, 1780 cm^{-1}, and 1819 cm^{-1} indicate assymetric stretch of the NHS carbonyls, symetric stretch of the NHS carbonyls, and activated ester carbonyl peaks, respectively. Assignment of peaks was based on assignments by Frey and Corn (Frey and Corn, *Anal Chem.* 68, 3187-3193, 1996).

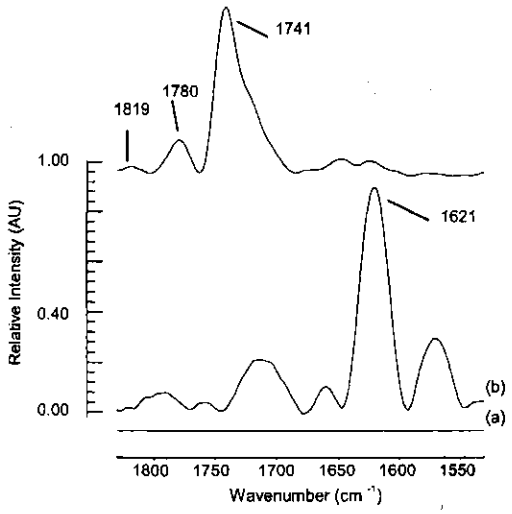

Fig. 8: PIERS spectra acquired for (a) EG_3 SAM; (b) mixed SAM of 95% EG_3 and 5% EG_6-COOH; (c) mixed SAM of 95% EG_3 and 5% EG_6-COOH following activation with NHS.

Ligand tethering onto mixed EG_3/EG_6-COOH SAMs was examined by ELISA. Bioactive peptides were synthesized with an additional spacer (KGGG) on the NH_2-terminus for tethering onto SAMs. Active NHS-esters are specific for free amines, ensuring that these peptides are tethered at their NH_2-terminus. In order to characterize the immobilization profiles for the peptides, each peptide was labeled with biotin at a cystine residue using maleimide chemistry. Bioactive ligands displayed similar immobilization behavior with an initial linear increase in ligand density with solution concentration, followed by saturating levels of immobilized peptide (**Fig. 9**). Only surfaces activated with the reactive NHS ester intermediate showed significant tethering of peptide. These results indicate that by varying the coating concentration of peptide, the amount tethered to the SAMs can be tightly controlled.

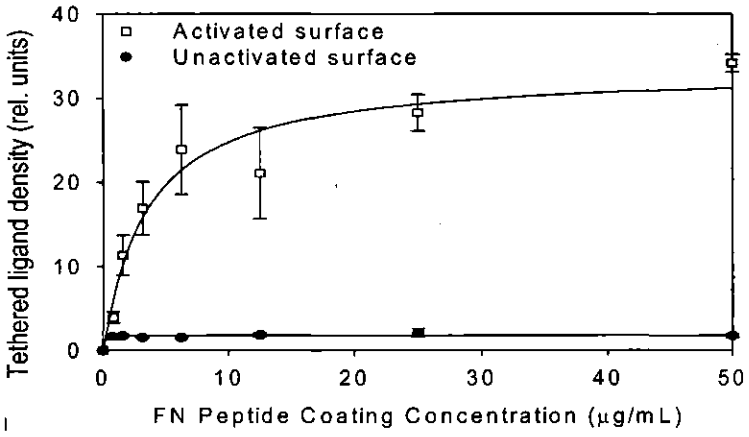

Fig. 9: Tethering profile of bioactive ligand to SAMs as a function of ligand coating concentration. SAMs not activated with NHS were unable to tether peptides while activated SAMs supported significant levels of ligand immobilization.

4. Surface-nucleated assembly of fibrillar ECMs

Biologically-inspired materials have emerged as promising substrates for enhanced repair in various therapeutic and regenerative medicine applications, including nervous and vascular tissues, bone, and cartilage (Lutolf and Hubbell, *Nat Biotech* 23, 47-55, 2005). These strategies focus on the development of materials which integrate well-characterized domains from biomacromolecules to mimic individual functions of the ECM, including cell adhesion, growth factor binding, and protease sensitivity. While these biomimetic materials imitate particular ECM attributes, they exhibit reduced activity compared to natural

matrices and often do not recapitulate the full spectrum of functions necessary for robust control of cell function associated with ECMs. A vital property of ECMs is the fibrillar architecture arising from supramolecular assembly. For example, the fibrillar structure of FN matrices modulates cell cycle progression, migration, gene expression, cell differentiation, and the assembly of other matrix proteins (Sechler and Schwarzbauer, *J Biol Chem* 273, 25533-25536, 1998; Sakai et al., *Nature* 423, 876-881, 2003). Current biomaterials, however, do not actively promote deposition and assembly of fibrillar, supramolecular structures characteristic of natural matrices.

By tethering an oligopeptide (FN13) from the self-assembly domain of fibronectin (FN) [2], we have engineered surfaces that nucleate the assembly of robust fibrillar FN matrices. Oligopeptides, including FN13 (KGGGAHEEICTTNEGVM), bioadhesive RGD (GRGDSPC), and control scrambled sequences (KGGGITCETNEGEVAMH), were selectively tethered onto self-assembled monolayers (SAMs) consisting of reactive carboxylic acid-terminated thiols and non-fouling oligo(ethylene glycol)-terminated (5% COOH-EG_6:EG_3) thiols. This allowed us to engineer surfaces that present controlled densities of peptide within a protein adsorption-resistant background. To examine the ability of these engineered supports to direct matrix assembly, cells were cultured on substrates functionalized with equimolar peptide densities (35 pmol/cm^2) in serum-containing media. Surfaces presenting FN13 supported assembly of robust fibrillar FN matrices surrounding adherent cells; while negligible FN fibrils were observed on surfaces presenting a control-scrambled sequence or on unmodified supports (**Fig. 10A**). Furthermore, the assembled matrices were not a simple consequence of the presence of adherent cells, since no fibrils were observed on RGD-functionalized supports (**Fig. 10A**).

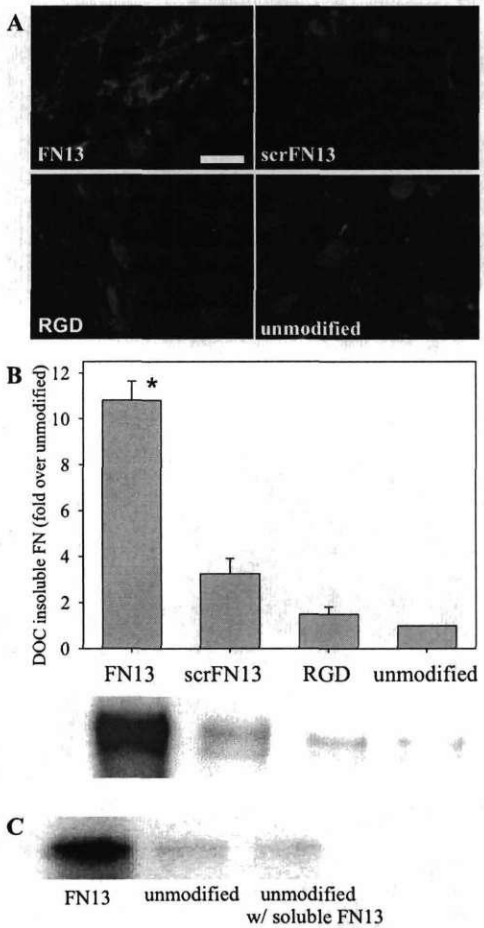

Fig. 10: FN13-functionalized surfaces direct robust FN matrix assembly. (A) Immunofluorescence staining of assembled FN matrix architecture (FN = red, DNA = blue, bar 10 μm). (B) DOC-insoluble assembled FN. * vs. scrFN13, RGD, and unmodified ($p < 0.00006$). (C) DOC-insoluble matrix for FN13-tethered, unmodified and soluble FN13 (40 μg/ml) on unmodified surfaces, showing requirement for FN13 immobilization.

During cell-mediated matrix assembly, FN is cross-linked into deoxycholate (DOC)-insoluble multimers. Biochemical analyses revealed ten-fold higher levels of DOC-insoluble FN on FN13-functionalized surfaces compared to control supports (**Fig. 10B**). FN assembly was entirely dependent on the presence of cells as no FN staining was evident on FN13-functionalized surfaces incubated in serum-containing media in the absence of cells. In addition, it was shown that the assembled matrix comprised FN synthesized by cells, and not FN incorporated from the serum-containing media. Finally, matrix assembly required immobilized FN13, as no FN fibrils were present on cultures exposed to soluble FN13 (**Fig. 10C**). Taken together, these results demonstrate surface-directed assembly of FN matrices with the structural and biochemical characteristics of native ECMs.

To gain further insights into surface-directed matrix assembly, FN assembly was analyzed as a function of FN13 surface density. Surprisingly, FN matrix assembly exhibited a threshold density-dependent response. Below a critical density (~ 8.9 fmol/cm^2), background levels of assembled FN were detected (**Fig. 11A**). Above this threshold density, >10-fold higher levels of assembled FN were observed, and no further increases in matrix assembly were obtained by further increasing the density

of FN13. This relationship between matrix assembly and FN13 density is consistent with a nucleation mechanism in which the spacing between FN13 molecules controls matrix assembly. A critical FN13 density of 9.0 fmol/cm^2 corresponds to an average FN13-FN13 spacing of 155 nm, which is larger that the dimensions for soluble, compact FN. Remarkably, this spacing is in excellent agreement with the dimensions of the linearly extended form of FN (160 nm) (**Fig. 11B**). We propose a model for surface-directed matrix nucleation in which tethered FN13 peptides bridge linearly extended FN conformers, which then mediate assembly of FN multimers. This model is consistent with the observed surface density-dependent effects. For large FN13-FN13 spacing (corresponding to lower surface densities), FN13 peptides cannot bridge the FN molecule and matrix assembly is not triggered. Conversely, FN13-FN13 spacings below the critical spacing do not increase matrix assembly because assembly is limited by the dimensions of the FN molecule.

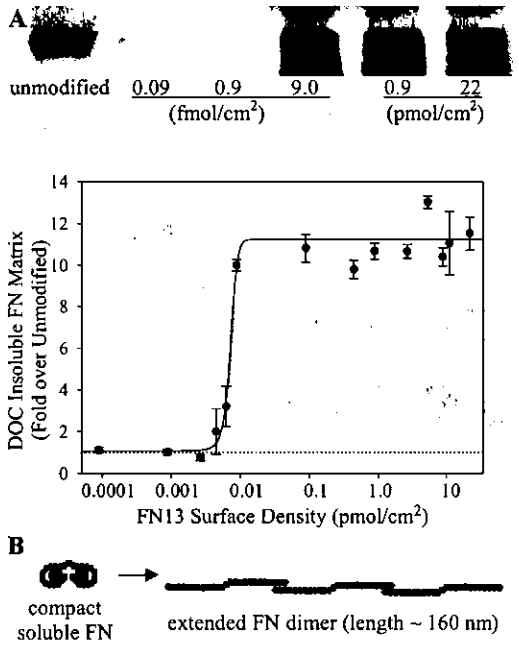

Fig.11: Critical FN13 density is required for nucleation of FN matrices. (A) DOC-insoluble FN matrix assembly as a function of FN13 surface density (hashed line represents values for unmodified surface). Curve fit to nonlinear regression ($R^2 = 0.97$). (B) Model for FN13-induced matrix assembly depicting FN extension from compact soluble conformer to linearly extended form associated with assembled FN fibrils (length ~ 160 nm).

To further analyze the bioactivity of these engineered surfaces, cell proliferation rates were examined. Cells cultured on FN13-functionalized surfaces displayed a two-fold enhancement in cell proliferation rate compared to RGD-presenting and control supports (**Fig. 12**). This result is in excellent agreement with the ability of assembled FN matrices to regulate cell cycle progression via modulation of proliferation rates [2]. The increases in cell proliferation rates on FN13-functionalized surfaces demonstrate that surface-nucleated assembly of FN matrices yields molecular assemblies that modulate cellular activities.

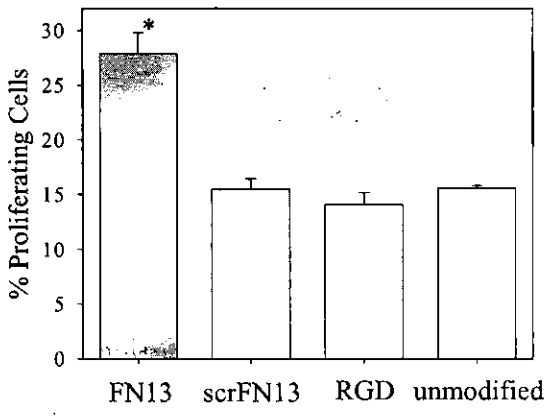

Fig.12: FN13-functionalized surfaces up-regulate cell proliferation rates. * vs. scrFN13, RGD, unmodified ($p < 0.0006$).

An important application of these matrix-nucleating surfaces is the ability to spatially control assembly of multiple ECM components. In addition to nucleating assembly of FN matrices, FN13-functionalized surfaces promoted assembly of type I collagen (COL) fibrils. Cells cultured on supports displaying FN13 directed assembly of COL within the FN fibrillar architecture (**Fig. 13A**). Image analysis of FN and COL matrices demonstrated excellent co-localization, indicating that the assembled FN matrix served as a template for the deposition of fibrillar COL. No collagen incorporation was observed on supports functionalized with RGD or scrambled FN13 sequence. Finally, micropatterning approaches were used to create FN13-functionalized patterns. Micropatterned domains presenting FN13 spatially controlled the assembly of FN matrices to distinct domains (**Fig. 13B**). FN matrix assembly was restricted to areas presenting FN13, while no FN fibrils were detected between functionalized regions.

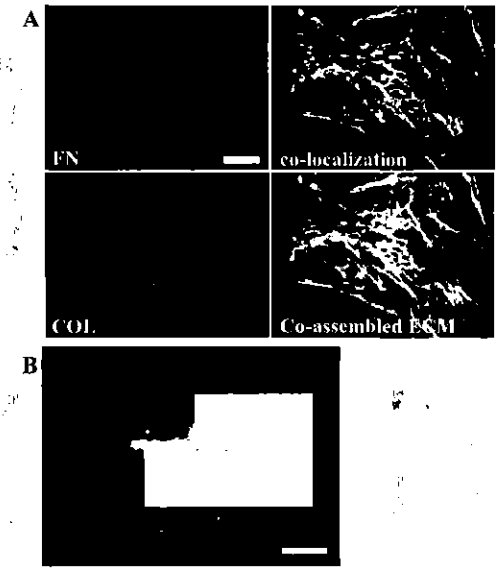

Fig.13: FN13 matrix-nucleating surfaces spatially control assembly of multiple ECM components. (A) Assembly of COL fibrils within FN13-nucleated FN matrices (FN=red, COL=green, DNA=blue, co-localization of FN & COL matrix = yellow; bar 10 μm). (B) Spatial control of assembled matrices using micropatterned substrates functionalized with FN13. FN13-functionalized lanes (10 μm wide, 50 μm spacing) induce localized FN matrix assembly (FN=red, DNA=blue, bar 20 μm).

In summary, we demonstrate that surfaces presenting an oligopeptide from the self-assembly domain of FN nucleate the assembly of robust fibrillar matrices that reproduce the structural and biochemical characteristics of native ECMs. These engineered FN matrices template the assembly of COL fibrils and up-regulate cell proliferation rates. Furthermore, by micropatterning the tethered peptide, spatial control of matrix assembly was demonstrated. These synthetic matrix-nucleating materials represent a promising biomimetic strategy to engineer bio-interactive materials for biotechnological and biomedical applications.

5. Integrin Binding Specificity Modulates Cell Adhesion and Signaling

We engineered a monobiotinylated FNIII7-10 by encoding a biotinylation sequence at the amine terminus of the protein. This fibronectin fragment represents an enhanced version of the previously described fragment with a single biotin tag introduced at a specific site not affecting the central cell binding domain. The expressed recombinant protein is biotinylated at a single, specific site and can be easily purified via affinity chromatography. In addition to providing a simple system to generate large quantities of purified protein via affinity chromatography (2-10 mg from 1 liter culture, >98% purity), this strategy incorporates a well-defined tag for tethering onto avidin supports as well as a tracking marker for future in vitro and in vivo studies. The biological activity of FNIII7-10 was demonstrated by ELISA using the HFN7.1 monoclonal antibody. This monoclonal antibody is which is specific for the central cell-binding domain in the 9th to 10th type III repeats of FN and blocks cell adhesion to FN.

Mixed alkanethiol SAMs were used as model surfaces presenting well-defined anchoring groups (COOH) for controlled covalent tethering of ligands in a protein adsorption-resistant background (EG_3). Peptides/ligands were tethered via free amines using NHS/EDC coupling chemistry previously used on SAMs (Capadona et al., *Adv Mater* 17, 2604-2608, 2005). The percentage of anchoring groups within the SAM is expected to be an important design parameter; high enough densities of anchoring groups are desired to afford for both a wide range of ligand densities, but at the same time, the anchoring group density must be low enough to preventing non-specific ligand adsorption. We examined FNIII7-10 tethering/adsorption onto activated/unactivated SAMs with EG_6-COOH:EG_3 solution ratios ranging from 0.0001 to 0.1 via ELISA. We determined that an EG_6-COOH:EG_3 solution ratio of 0.02 yielded the highest tethered ligand density while maintaining background levels of non-specific adsorption. Higher ratio surfaces produced only slightly higher peptide surface density, but much higher levels of background non-specific adsorption. This model system presents a well-defined surface with a single adhesive ligand that allows direct functional comparison on a molar basis among different adhesive ligands.

Three adhesive ligands were examined: (i) RGD peptide (GRGDSPC); (ii) RGD-PHSRN peptide ($GRGDG_{13}PHSRN$) presenting the RGD and PHSRN motifs joined by a random conformation polyglycine sequence designed to mimic the spacing of the domains in FN, but not interfere with the adhesion characteristics of the two linked sequences (Benoit and Anseth, *Biomaterials* 26,5209-5220, 2005); and (iii) FNIII7-10. Quantification of ligand tethering onto SAMs was conducted via SPR. Tethered ligand surface density increased hyperbolically with coating concentration, reaching saturation levels at higher concentrations (~5 μg/ml for FNIII7-10, ~30 μg/ml for RGD, RGD-PHSRN) (**Fig. 14A**). This data indicate that control over tethered peptide density can be achieved by varying coating concentration accordingly. Although the tethering curves exhibited similar hyperbolic shapes, RGD and RGD-PHSRN tethered at >10-fold higher molar densities than FNIII7-10 (**Fig. 14A**). Tethered ligands were biologically active as determined by cell spreading. At saturated surface densities, all engineered surfaces exhibited equivalent levels of cell spreading, while very few cells attached to EG_3 or unactivated EG_6-COOH: EG_3 surfaces (**Fig. 14B**).

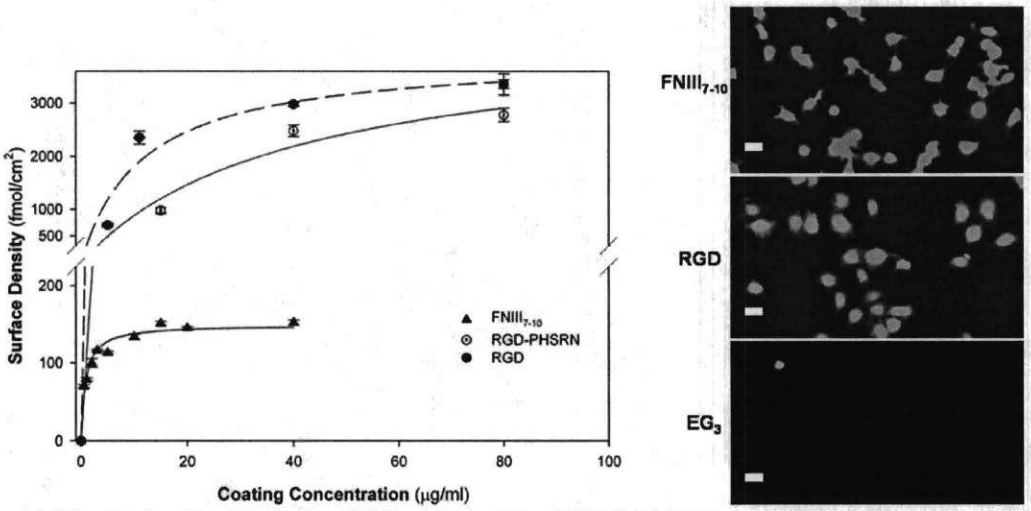

Fig. 14: Bioadhesive ligand tethering. (**A**) Surface density of FNIII7-10, RGD, and RGD-PHSRN tethered to 2% EG_6-COOH:EG_3 SAM surfaces as a function of coating concentration as determined by SPR (mean ± standard deviation; hyperbolic curve fit: RGD, $R^2 = 0.95$; RGD-PHSRN, $R^2 = 0.95$, FNIII7-10, $R^2 = 0.97$); (**B**) Images of calcein-labeled MC3T3-E1 cells adhering to peptide-tethered SAM surfaces for 1 h. Overall spreading and adhesion were similar on each peptide-tethered surface whereas few cells attached to EG3-terminated controls (Scale bars = 20 μm).

To further characterize the adhesive activities of these engineered biointerfaces, we measured the adhesion strength of MC3T3-E1 cells using a centrifugation assay that applies controlled detachment forces to adherent cells (Reyes and García, *J Biomed Mater Res* 67A, 328-333, 2003). Cells were seeded for 1 h in serum-containing media and then centrifuged at 57g for 5 min. For all surfaces, the fraction of adherent cells increased sigmoidally with adhesive ligand surface density (**Fig. 15**), and adhesion strength was characterized as the ligand density required for half-maximal adhesion (ADH50). Adhesion strength is inversely related to ADH50, as a shift of the curve left (decreasing ADH50) represents an increase in adhesion strength since less ligand is needed for cell adhesion. Cell adhesion profiles for RGD- and RGD-PHSRN-tethered surfaces were almost identical (ADH50 values were 2300 and 1950 fmol/cm2, respectively), indicating similar adhesive activity for these two peptides. FNIII7-10-tethered surfaces exhibited higher adhesion levels on saturated density surfaces, and also displayed a pronounced leftward shifted adhesion profile compared to the other two peptide tethered-surfaces. These data indicate that the FNIII7-10-tethered surface displays higher cell adhesive activity compared to RGD or RGD-PHSRN-tethered surfaces at each molar density.

We then examined whether these different adhesive surfaces supported cell adhesion by binding different integrin receptors. Function-perturbing antibodies directed against different integrin subunits were

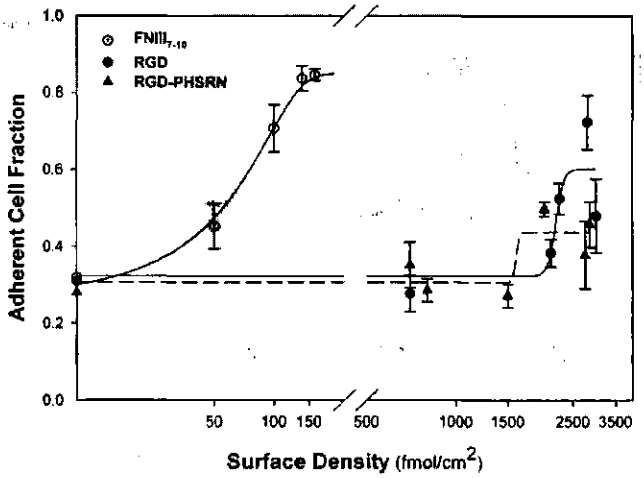

Fig. 15: MC3T3-E1 cell adhesion strength to SAMs presenting controlled densities of bioadhesive ligands (1 h adhesion, centrifugation at 57 g for 5 min). FNIII7-10 cell adhesion strength profile is shifted upward and leftward, indicating an increase in adhesion strength over RGD and RGD-PHSRN-tethered surfaces (mean ± standard error, n = 5; sigmoidal curve fits: RGD, R^2 = 0.80; RGD-PHSRN, R^2 =0.79; FNIII7-10, R^2 = 0.96).

used to block adhesion to the engineered interfaces. Since integrins $\alpha_5\beta_1$ and $\alpha_v\beta_3$ represent the dominant adhesion receptors for FN in MC3T3-E1 cells, we analyzed the contributions of these receptors to adhesion strength on the peptide-functionalized SAMs. Surfaces were tethered with maximum density of ligand (according to SPR curves), and the relative cell adhesion was normalized to unblocked controls samples. Blocking antibodies directed against $\alpha_5\beta_1$ integrin reduced adhesion to background levels (EG_3) for the FNIII7-10-tethered surface, but only slightly reduced adhesion on the RGD and RGD-PHSRN surfaces (**Fig. 16**). In contrast, antibodies against the β_3 integrin subunit did not alter adhesion significantly for FNIII7-10-tethered surfaces, but reduced adhesion over 75% for both the RGD and RGD-PHSRN surfaces. These results demonstrate that the FNIII7-10-tethered surface primarily supports $\alpha_5\beta_1$-mediated adhesion, whereas the RGD- and RGD-PHSRN-functionalized surfaces promote $\alpha_v\beta_3$-mediated cell adhesion.

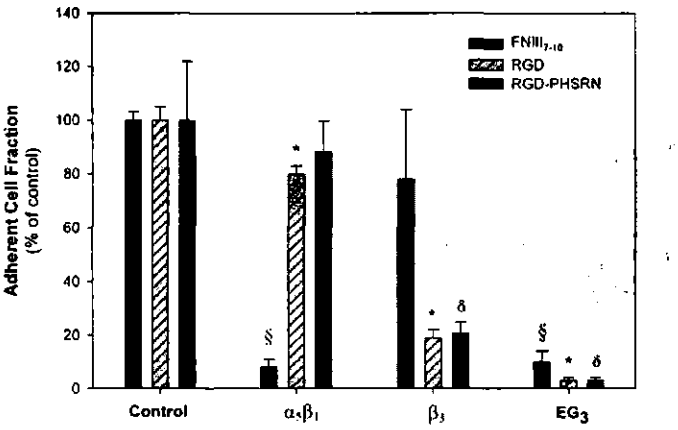

Fig. 16: Surfaces presenting FNIII7-10 display integrin binding specificity compared to RGD supports. Blocking antibodies against integrin α5β1 completely inhibited cell adhesion to FNIII7-10 surfaces (§ vs. control, $p<0.0009$) and, to a much lesser extent, the RGD surface (* vs. RGD control, $p<0.01$). In contrast, blocking β3 blocked cell adhesion only to the RGD (* vs. control, $p<0.0009$) and RGD-PHSRN (δ vs. control, $p<0.0009$) surfaces. Adhesion to peptide-incubated EG_3 control surfaces was minimal. Results are expressed as percent inhibition compared to unblocked cell control (mean ± standard error, 3 independent experiments with n = 8).

Since MC3T3-E1 cells assemble robust focal adhesions containing clustered integrins and intracellular structural and signaling proteins, we examined integrin binding and focal adhesion assembly on the engineered interfaces by staining for different integrin subunits and vinculin, an intracellular structural protein which localizes to focal adhesions. Cells adhering to FNIII7-10-tethered surfaces displayed robust, well-defined adhesive structures containing $\alpha_5\beta_1$ integrins but minimal $\alpha_v\beta_3$ binding. Cells on RGD-tethered surfaces exhibited clustering of $\alpha_v\beta_3$ and little staining for $\alpha_5\beta_1$. These results further confirm the antibody blocking results and demonstrate further that surfaces presenting FNIII7-10 primarily support $\alpha_5\beta_1$-mediated adhesion, while RGD-functionalized SAMs mediate adhesion via $\alpha_v\beta_3$.

We next determined whether these bioadhesive interfaces modulated intracellular signaling and high-order cell activities. We analyzed levels of focal adhesion kinase (FAK) phosphorylation as a marker of integrin-mediated signaling. We probed for phosphorylation of important tyrosine residues using site-specific antibodies in Western blotting. Phosphorylation of tyrosine-397, the autophosphorylation site on FAK which also binds to the p85 subunit of PI3-kinase, was increased almost threefold on the FNIII7-10

surface compared to the RGD-tethered surface at maximum peptide densities (**Fig. 17**). Similarly, phosphorylation of tyrosine-576, located in the FAK catalytic loop and responsible for maximal FAK kinase activity, was significantly higher on the FNIII7-10-tethered surface compared to the RGD-functionalized support. Because integrin-mediated activation of FAK has been linked to upregulation of cell proliferation, we investigated whether adhesion to the different biointerfaces would modulate MC3T3-E1 proliferation. The proliferation rate of cells seeded for 16 h on each ligand-tethered surface was probed by BrdU incorporation (4 h). Cells seeded on FNIII7-10-functionalized surfaces displayed a two-fold increase in cell proliferation rate compared to RGD-tethered surfaces at low and high relative peptide surface densities (**Fig. 18**), underlining the significance of integrin specificity on particular cellular functions.

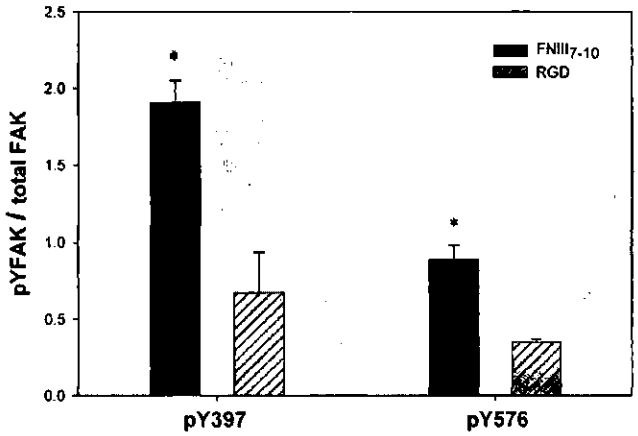

Fig. 17: Phosphorylation of site-specific tyrosine residues of FAK in MC3T3-E1 seeded cells on saturated density RGD and FNIII7-10-tethered surfaces (3000 and 150 fmol/cm2, respectively). Quantification of Western blot band intensity demonstrating higher phosphorylation of Tyr-397 ($p<0.006$) and Tyr-576 ($p<0.001$) on FNIII7-10 over RGD-tethered surfaces (Mean ± standard error, n=6). Intensities for phosphorylated FAK were normalized to total FAK.

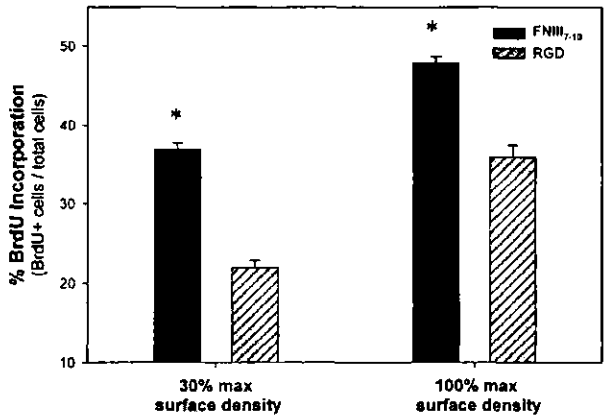

Fig. 18: Proliferation rate (% BrdU+ cells, mean ± standard error) for MC3T3-E1 cells cultured for 20 h on RGD and FNIII7-10-tethered surfaces for two different peptide densities. FNIII7-10-tethered surfaces display higher proliferation rate compared to RGD supports for both saturated (150 and 3000 fmol/cm2; $p<0.01$) and sub-saturated (45 and 1150 fmol/cm2; $p<0.001$) densities.

6. Micropatterned Surfaces to Direct α5β1 Integrin-Mediated Adhesion

We have engineered micropatterned surfaces that present integrin-specific ligands. Microcontact printing of alkanethiol mixtures (1% COOH-EG_6:EG_3) onto Au supports was used to generate micropatterned islands (20 μm diameter circles, 75 μm center-center spacing). Bare Au areas were functionalized with EG_3-terminated thiol to render them non-fouling and non-adhesive. FNIII7-10 was then tethered onto micropatterned domains following NHS/EDC activation of the COOH anchors. Processing parameters (stamp pressure, stamp time, FNIII7-10 concentration) were varied to generate micropatterned islands presenting tethered FNIII7-10 (**Fig. 19**). Cells seeded on these surfaces individually adhered to the

micropatterned domain and remained constrained to the island. We are currently analyzing cell adhesive and signaling responses to these materials.

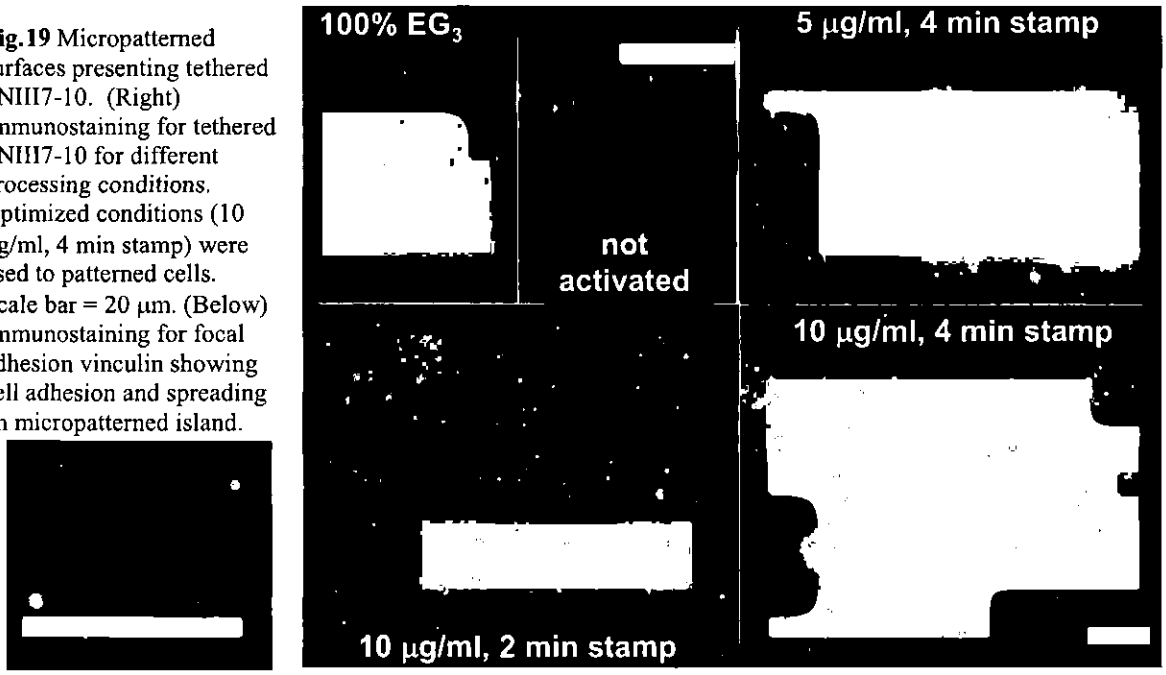

Fig.19 Micropatterned surfaces presenting tethered FNIII7-10. (Right) Immunostaining for tethered FNIII7-10 for different processing conditions. Optimized conditions (10 μg/ml, 4 min stamp) were used to patterned cells. Scale bar = 20 μm. (Below) Immunostaining for focal adhesion vinculin showing cell adhesion and spreading on micropatterned island.

Educational and Outreach Activities

We developed a middle school science Web-based module on receptor-ligand interactions ("Receptor Guy"). The module, written in Macromedia's Director, has been packaged as a Flash file on CD-ROMs and distributed to several middle-school science teachers in local public and private schools for initial feedback and evaluation. We met with several middle-school science teachers from Atlanta Public School and Dekalb County School districts and obtained feedback on improvements to the module and content for future modules. The Georgia Public School Science curriculum is currently undergoing a major evaluation and we are discussing implementation of these modules into the curriculum. We have identified several challenges to integrating the module into the science curriculum including teacher training and support, wide distribution of modules, integration into coursework, and manpower and resources associated with the development and implementation of these modules. We have also discussed the possibility of creating "hands on" kits or demonstration units to complement science courses. These kits offer significant advantages compared to the modules in terms of simplicity and impact. We have also met with representatives from the Fernbank Museum of Natural History to discuss possible integration of our research into their science and outreach programs. Both the middle-school teachers and Fernbank representatives were excited by the idea of creating kits or demonstration units to complement science courses. In addition to these science kits, we are currently discussing creating a one-week science camp module focusing on biomaterials. This module would provide hands-on and problem-based learning experiences for middle school students. Finally, during this project, we actively provided educational training to several undergraduate (REU as well as other students) and graduate students.